

Disambiguation of Human Intent Through Control Space Selection

Deepak E. Gopinath* · Brenna D. Argall

Received: date / Accepted: date

Abstract Assistive shared-control robots have the potential to transform the lives of millions of people afflicted with severe motor impairments as a result of spinal cord or brain injuries. The effectiveness and usefulness of shared-control robots is closely related to their ability to infer the user’s needs and intentions and is often a limiting factor for providing appropriate assistance quickly, confidently and accurately. The contributions of this paper are three-fold: first, we propose a goal disambiguation algorithm which enhances the intent inference and assistive capabilities of a shared-control assistive robotic arm. Second, we introduce a novel intent inference algorithm that works in conjunction with the disambiguation scheme, inspired by *dynamic field theory* in which the time evolution of the probability distribution over goals is specified as a dynamical system. Third, we present a pilot human subject study to evaluate the

efficacy of the disambiguation system. This study was performed with eight subjects. Our results suggest that (a) the disambiguation system has a greater utility value as the control interface becomes more limited and the task becomes more complex, (b) subjects demonstrated a diverse range of disambiguation request behavior with a greater concentration in the earlier parts of the trial and (c) there are no differences in the onset of robot assistance between different mode switching paradigms across tasks or across interfaces.

Keywords Shared Autonomy · Intent Inference · Intent Disambiguation · Assistive Robotics

1 Introduction

Assistive and rehabilitation machines—such as robotic arms and smart wheelchairs—have the potential to transform the lives of millions of people with severe motor impairments (LaPlante et al 1992). These machines can promote independence, boost self-esteem and help to extend the mobility and manipulation capabilities of such individuals, and revolutionize the way motor-impaired people interact with society (Scherer 1996; Huete et al 2012). With rapid technological strides in the domain of assistive robotics, the machines have become more capable and complex, and with this complexity the control of these machines has become a greater challenge.

The control of an assistive machine is typically enacted through a control interface. Moreover, the greater the motor impairment of the user, the more limited are the interfaces available for them to use. These interfaces (for example, sip-and-puffs and switch-based head arrays) are low-dimensional, discrete interfaces that can operate only in subsets of the entire control

This material is based upon work supported by the National Science Foundation under Grant CNS 1544741. Any opinions, findings and conclusions or recommendations expressed in this material are those of the authors and do not necessarily reflect the views of the aforementioned institutions.

Deepak E. Gopinath
Department of Mechanical Engineering
Northwestern University, Evanston, IL
Shirley Ryan AbilityLab, Chicago, IL.
Phone No: +12013109061
E-mail: deepakgopinath@u.northwestern.edu

Brenna D. Argall
Department of Mechanical Engineering, Department of Electrical Engineering and Computer Science, Northwestern University, Evanston, IL.
Department of Physical Medicine and Rehabilitation, Northwestern University, Chicago, IL,
Shirley Ryan AbilityLab, Chicago, IL.
E-mail: brenna.argall@northwestern.edu

* Corresponding Author

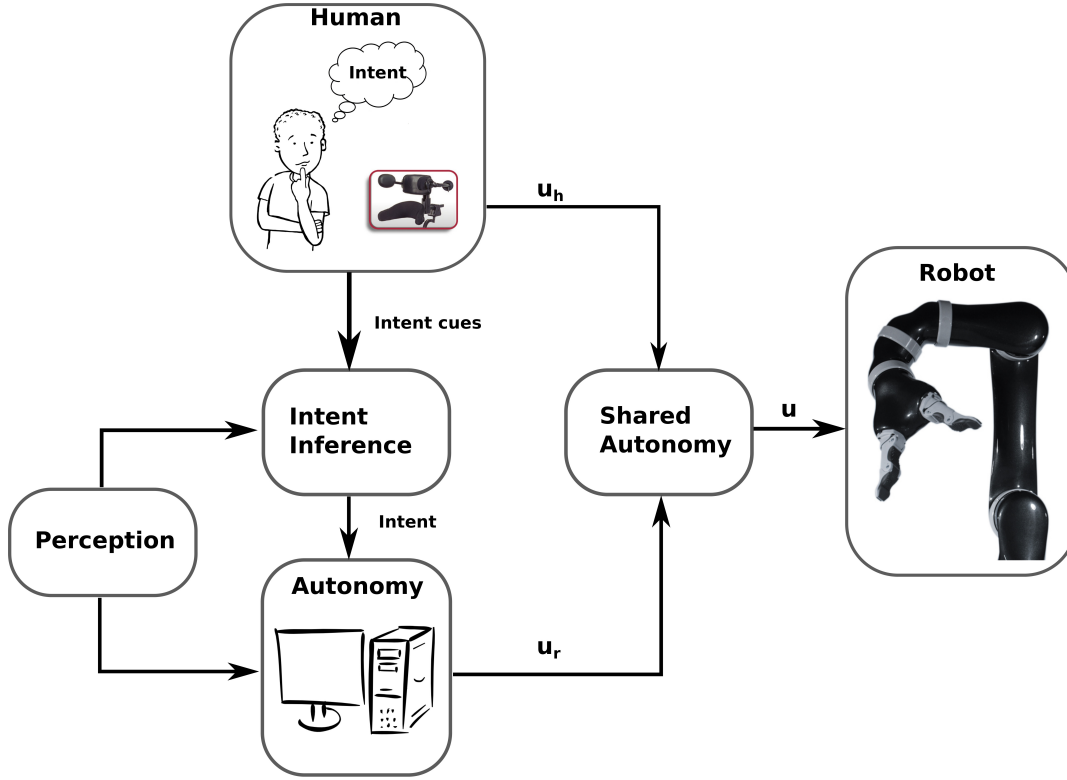


Fig. 1 Illustration of the core components of a shared control architecture. u_h denotes the human control command, u_r denotes the autonomy control command and u is the final control command issued to the robot. The intent inference module can extract intent cues from the human in multiple ways, for example via the human control actions or biometric measures that indicate the cognitive and physical load of the user during task execution. In our work we intentionally restrict this to be similar to operating the machine without autonomy and so intent information is u_h exclusively.

space (Simpson et al 2008; Nuttin et al 2002). The dimensionality mismatch between the control interfaces and the controllable degrees-of-freedom of the assistive robot necessitates the partitioning of the entire control space into smaller subsets called *control modes*. Moreover, the more limited and lower-dimensional the control interface, the greater the number of control modes. In order to achieve full control of the machine, the user must switch between the control modes, which is referred to as *mode switching* or *modal control*. Mode switching adds to the cognitive and physical burden of task execution and has a detrimental effect on the performance (Eftring and Boschian 1999). The introduction of *shared autonomy* to these assistive machines seeks to alleviate some of these issues. In a shared control system the task responsibility is shared between the user and the robot, with the aim of reducing human effort in achieving a goal. Shared autonomy systems arbitrate between the human control commands and the autonomous control commands using different strategies depending on the task context, user

preference and robotic platform. Figure 1 depicts the key components of a typical shared control architecture.

Any assistive robotic system needs to have a good idea of the user’s needs and intentions. Therefore, intent inference is a necessary and crucial component to ensure appropriate assistance. In assistive robotic manipulation specifically, often the first step of a manipulation task is to reach for and grasp discrete objects in the environment. Intent inference therefore can be framed as a problem of estimating a probability distribution of intent likelihood over all possible goals (objects) in the environment. This inference is usually informed by various cues from the human and the environment, such as the human control actions, biometric measures that indicate the cognitive and physical load of the user during task execution and task-relevant features such as robot and goal locations. With a greater number of sensor modalities available, it is likely that the intent inference becomes more accurate.

However, in the assistive domain, user acceptance and adoption is of paramount importance. Adding more

sensors to track biometric data and object locations can become expensive or impractical (e.g. if the sensor must be worn by the user). For reasons of user adoption and cost, we intentionally design our assistance add-ons to be as invisible and close to the manual system as possible. The information we are able to capture from the human therefore is largely restricted to the control commands they issue to the assistive machine. Sparsity and noise in these control commands make the inference task even harder, prompting the need for robust intent inference formalisms.

Our key insight is that certain control commands issued by the human are *more intent expressive* than others, and may help the autonomy in inference accuracy. This is the notion of *inverse legibility* (Gopinath and Argall 2017) in which human-generated actions *help the robot* to infer the human’s intent unambiguously. Consider the hypothetical reaching experiment illustrated in Figure 2. Since the spatial locations of the goals are maximally spread along the horizontal axis, any human control command issued along the horizontal dimension conveys a lot of information about the intended goal to the robot. In other words, motion along x is more *intent expressive* and will help the robot to draw accurate inference more quickly and confidently. This approach to more seamless human-robot interaction exploits the underlying implicit exchanges of information between partners that are inherent to task execution with shared intentions.

In this work, as our primary contribution we develop a mode switch assistance paradigm that enhances the robot’s intent inference capabilities, by selecting the control mode in which a user-initiated motion will *maximally disambiguate* human intent. The disambiguation layer elicits more *intent expressive* commands from the user by placing the user control in certain control modes. Furthermore, the disambiguation power of the algorithm is closely linked to, and is dependent on, the success and accuracy of the underlying intent inference mechanism. Therefore, as our secondary contribution, we also develop a novel intent inference scheme which utilizes ideas from *dynamic field theory* that efficiently incorporates information contained in past states to improve the performance of the disambiguation system.

In Section 2 we present an overview of relevant research in the areas of shared autonomy in assistive robotics, types of shared autonomy assistance paradigms, intent inference and synergies in human-robot interaction. Section 3 presents the mathematical formalism developed for intent inference and disambiguation. Section 4 focuses on the implementation details of the shared control system. The study design and experimental methods are discussed in Section 5 followed by results

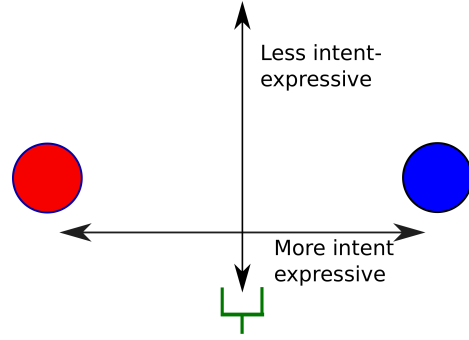


Fig. 2 Illustration of goal disambiguation along various control dimensions. Any motion of the end effector (green) along the y-axis will not help the system to disambiguate the two goals (A and B). However, motion along the x-axis provides cues as to which goal.

in Section 6. Discussion and conclusions are presented in Sections 7 and 8 respectively.

2 Related Work

This section provides an overview of related research in the domains of shared autonomy in assistive robotics, robot assistance for modal control, intent inference in human-robot interaction and information acquisition in robotics.

Shared-autonomy in assistive systems aims to reduce the user’s cognitive and physical burden during task execution without having the user relinquish complete control (Philips et al 2007; Demeester et al 2008; Gopinath et al 2017; Muelling et al 2017). The most common strategies to share control between the user and the assistive system include (a) hierarchical paradigms in which the higher level goals are entrusted with the user and the autonomy generates low-level control (Tsui et al 2011; Kim et al 2010, 2012), (b) control allocation in distinct partitions of the control space (Driessen et al 2005) and (c) blending user controls and robot autonomy commands (Downey et al 2016; Storms and Tilbury 2014; Muelling et al 2017).

In order to offset the drop in task performance due to shifting focus (task switching) from the task at hand to switching between different control modes different mode switch assistance paradigms have been proposed. For example, a simple time-optimal mode switching scheme has shown to improve task performance (Herlant et al 2016; Pilarski et al 2012).

Shared control systems often require a good estimate of the human’s intent—for example, their intended reaching target in a manipulation task or a target location in the environment in a navigation task (Liu et al 2016). Intent can either be explicitly communi-

cated by the user (Choi et al 2008) or can be inferred from their control signals or sensor data using various algorithms. Intent recognition and inference are actively studied by cognitive scientists and roboticists and can be broadly categorized into two main classes: model-based approaches and heuristic approaches. In model-based approaches, intent inference is typically cast within a Bayesian framework, and the posterior distribution over goals (belief) at any time is determined by the iterative application of Bayes theorem. Evidence in this context can be derived from a combination of factors such as task-relevant features in the environment, human control actions or biometric data from the user (Baker et al 2007, 2009). The user often is modeled as a Partially Observable Markov Decision Process (POMDP) (Taha et al 2011) and is assumed to behave according to a predefined control policy that maps the states to actions. Although iterative belief updating using Bayes theorem provides an optimal strategy to combine new evidence (likelihood) with *a priori* information (prior), incorporating an extended history of past states and control actions increases the computational complexity and tractability becomes an issue. In such cases, first-order Markovian independence assumptions make the inference tractable. In heuristic approaches, the formulations are often simpler and seek to find direct mappings from instantaneous cues and the underlying human intention. For example, the use of instantaneous confidence functions for estimating intended reaching target in robotic manipulation (Dragan and Srinivasa 2012; Gopinath et al 2017). However, heuristic methods in general are not sophisticated enough to incorporate histories of past states and actions, making them less robust to external noise.

Eliciting more legible and information-rich control commands from the user to improve intent estimation can be thought of as an information acquisition process. Intent information acquisition can be an *active* process in which the robot takes actions that will probe the human’s intent (Sadigh et al 2016b,a). Designing optimal control laws that maximize information gain can be accomplished by having the associated reward structure reflect some measure of information gain (Atanasov et al 2014). Autonomous robots designed for exploration and data acquisition tasks can benefit from exploring more information-rich regions in the environment. If the spatial distribution of information density is known *a priori*, information maximization can be accomplished by maximizing the ergodicity of the robot’s trajectory with respect to the underlying information density map (Miller et al 2016; Miller and Murphey 2013).

By having the human assist the robot in its intent inference capacity, our work leverages the underlying

synergies that are inherent in human-robot cooperation. In the context of human-human cooperative teams, the notion of shared intentionality—one in which all parties involved in a collaborative task team share the same intention or goal and have a joint commitment towards it—is crucial to make task execution more seamless and efficient (Tomasello and Carpenter 2007; Tomasello and Moll 2010). This principle is relevant to successful human-robot interaction as well. From the robot’s perspective, the core idea behind our disambiguation system is that of “*Help Me, Help You*”—that is, if the user can help the robot with more information-rich actions, then the robot in turn can provide accurate and appropriate task assistance more quickly and confidently. A framework for “*people helping robots helping people*” in which the robot relies on semantic information and judgments provided by the human to improve its own capabilities has been developed in (Sorokin et al 2010). In order to overcome the various types of communication bottlenecks that can hamper performance, different types of communication interfaces have been developed that account for the restricted capabilities of the robot (Goodfellow et al 2010). Lastly, more intent-expressive human actions is related to the idea of legibility in robot actions. In human-robot interaction, the legibility and predictability of robot motion to the human has been investigated (Dragan et al 2013) and various techniques to generate legible robot motion have been proposed (Holladay et al 2014). Our work introduces the idea of *inverse legibility* (Gopinath and Argall 2017) in which the assistance scheme is intended to bring out more legible intent-expressive control commands *from* the human.

3 Mathematical Formalism

This section describes our intent disambiguation algorithm that computes the control mode that can maximally disambiguate between the goals and the intent inference mechanism that works in conjunction with the disambiguation algorithm. Section 3.1 outlines the mathematical notation used in this paper. Section 3.2 describes the disambiguation algorithm. The mathematical details of the intent inference paradigms is outlined in detail in Section 3.3.

3.1 Notation

Let \mathcal{G} denote the set of all candidate goals with $n_g = |\mathcal{G}|$ and let g^i refer to the i^{th} goal with $i \in [1, 2, \dots, n_g]$. A *goal* represents the human’s underlying intent. Specifically, in assistive robotic manipulation, since the robotic

device is primarily used for reaching toward and grasping of discrete objects in the environment, intent inference is the estimation of the probability distribution over all possible goals (objects) in the environment. At any time t , the robot actively maintains a probability distribution over goals denoted by $\mathbf{p}(t)$ such that $\mathbf{p}(t) = [p^1(t), p^2(t), \dots, p^{n_g}(t)]^T$ where $p^i(t)$ denotes the probability associated with goal g^i . The probability $p^i(t)$ represent the robot's *confidence* that goal g^i is the human's intended goal.

Let \mathcal{K} be the set of all controllable dimensions of the robot and k^i represent the i^{th} control dimension where $i \in [1, 2, \dots, n_k]$. The cardinality of \mathcal{K} is denoted as n_k and typically depends on the robotic platform used. For example, for a smart wheelchair $n_k = 2$, since the controllable degrees-of-freedom are velocity and heading and for a six degrees-of-freedom robotic arm with a gripper $n_k = 7$.

The limitations of the control interfaces necessitate the control space \mathcal{K} to be partitioned into control modes. Let \mathcal{M} denote the set of all control modes with $n_m = |\mathcal{M}|$. Additionally, let m^i refer to the i^{th} control mode where $i \in [1, 2, \dots, n_m]$. Each control mode m^i is a subset of \mathcal{K} such that $\bigcup_{i=1}^{n_m} m^i$ spans all of the controllable dimensions.¹ Let \mathbf{e}^i be the standard basis vectors that denote the unit velocity vector along the i^{th} control dimension.² The disambiguation formalism developed in Section 3.2 is agnostic to the particular form of intent inference. However, the algorithm assumes that $\mathbf{p}(t)$ can be forward projected in time by iteratively applying the intent inference algorithm.

The disambiguation metric that characterizes the disambiguation capabilities of a control dimension $k \in \mathcal{K}$ is denoted by $D_k \in \mathbb{R}$. We explicitly define disambiguation metrics for both positive negative motions along k as D_k^+ and D_k^- respectively. We also define a disambiguation metric $D_m \in \mathbb{R}$ for each control mode $m \in \mathcal{M}$. D_m is a measure of how informative and useful the user control commands would be for the robot if the user were to operate the robot in control mode m . The higher it is, the easier it will be for the system to infer human's intent. Both D_k and D_m will be formally defined in Section 3.2.2.

The robot pose and the goal pose for $g \in \mathcal{G}$ are denoted \mathbf{x}_r and \mathbf{x}_g respectively and \mathbf{u}_h denotes the human control command.

3.2 Intent Disambiguation

The need for intent disambiguation arises from how the probability distribution over goals evolves as the user controls the robot and moves it in space. That is, given an intent inference mechanism that is dependent on robot pose or movement (Kelley et al 2008; Wang et al 2013), as the user controls the robot in different control modes, the probability distribution evolves.³ Figure 3 shows simulations which motivate the development of a disambiguation metric. For different control modes, the confidences associated with each goal are different. Moreover, motions in some control modes result in sharper rise in some goal confidences compared to others. This indicates the existence of control modes that can better disambiguate between the goals.

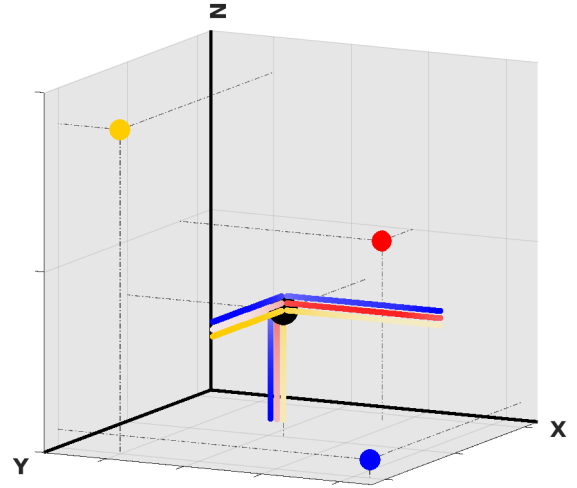


Fig. 3 Illustration of how goal confidences change upon motion along control dimensions. The three colored lines along each dimension represent the confidences associated with a goal of corresponding color. Brighter and dimmer colors correspond to high and low confidences respectively. One can see that motion along certain control dimensions results in sharper rise in confidences for some goals compared to others.

The computation of D_k depends on four components (denoted as Γ_k , Ω_k , Λ_k and Υ_k), which in turn depend on a projection of the probability distribution over intent. These projection and computations are described in detail in Section 3.2.1 and Section 3.2.2, and as a pseudocode in Algorithm 1.

¹Note that a dimension $k \in \mathcal{K}$ can be an element of multiple control modes.

²For the rotational control dimensions, the velocity is specified with respect to the end-effector of the robotic frame.

³Different approaches for intent inference that do *not* depend on robot motion or pose exist as well. For example, those that depend on eye gaze, electromyographic signals and brain signals.

Algorithm 1 Calculate $\mathbf{p}(t_b)$, $\mathbf{p}(t_c)$

Require: $\mathbf{p}(t_a), \mathbf{x}_r(t_a), \Delta t, t_a < t_b < t_c, \Theta$

```

1: for  $k = 0 \dots n_k$  do
2:   Initialize  $D_k = 0$ ,  $t = t_a$ 
3:   while  $t \leq t_c$  do
4:      $\mathbf{p}_k(t + \Delta t) \leftarrow \text{UpdateIntent}(\mathbf{p}_k(t), \mathbf{u}_h; \Theta)$ 
5:      $\mathbf{x}_r(t + \Delta t) \leftarrow \text{SimulateKinematics}(\mathbf{x}_r(t), \mathbf{u}_h)$ 
6:     if  $t = t_b$  then
7:       Compute  $\Gamma_k, \Omega_k, \Lambda_k$ 
8:     end if
9:     if  $t = t_c$  then
10:      Compute  $\Upsilon_k$ 
11:    end if
12:     $t \leftarrow t + \Delta t$ 
13:  end while
14:  Compute  $D_k$ 
15: end for

```

3.2.1 Forward Projection of $\mathbf{p}(t)$

The first step towards the computation of D_k is the forward projection of the probability distribution $\mathbf{p}(t)$ from the current time t_a to t_b and t_c ($t_a < t_b < t_c$), Algorithm 1, lines 3-13). We consider two projection times (t_b and t_c) in order to compute short-term and long-term behavior and evolution of the probability distribution. Application of control command \mathbf{e}^k results in probability distributions $\mathbf{p}_k^+(t_b)$, $\mathbf{p}_k^+(t_c)$ and $-\mathbf{e}^k$ results in $\mathbf{p}_k^-(t_b)$ and $\mathbf{p}_k^-(t_c)$. Note that Algorithm 1 is run twice to compute the projected probability distributions for \mathbf{e}^k and $-\mathbf{e}^k$.

The exact computation of the projected probability distribution will depend on the underlying intent inference computation—for example, whether it depends on \mathbf{x}_r (which can be computed from \mathbf{e}^k applied to the robot kinematics model) or \mathbf{u}_h (which can be taken as \mathbf{e}^k). All parameters and features which affect the computation of $\mathbf{p}(t)$ are denoted as Θ .

3.2.2 Components of D_k

The computation of disambiguation metric D_k consists of four components. Each of the following components encodes some aspect of the shape of the probability distribution and is computed for projections along both positive and negative directions independently. The four components are computed in lines 7 and 10 in Algorithm 1.

1) *Maximum probability:* The maximum of the projected probability distribution $\mathbf{p}_k(t_b)$ is a good measure of the robot’s overall certainty in accurate predicting human intent (The maximum of this discrete probability distribution is the mode of the distribution). A higher value implies that the robot has a good idea of which goal is the human’s intended goal. We define the

distribution maximum as Γ_k .

$$\Gamma_k = \max_{1 \leq i \leq n_g} p_k^i(t_b) \quad (1)$$

2) *Difference between largest probabilities:* Disambiguation accuracy benefits from greater differences between the first and second most probable goals. This difference is denoted as Ω_k .

$$\Omega_k = \max(\mathbf{p}_k(t_b)) - \max(\mathbf{p}_k(t_b) \setminus \max(\mathbf{p}_k(t_b))) \quad (2)$$

3) *Pairwise separation of probabilities:* If the difference between the largest probabilities fails to disambiguate, then the separation, Λ_k , in the remaining goal probabilities will further aid in intent disambiguation. The quantity Λ_k is computed as the *sum of the pairwise distances* between the n_g probabilities.

$$\Lambda_k = \sum_{i=1}^{n_g} \sum_{j=i}^{n_g} |p_k^i(t_b) - p_k^j(t_b)| \quad (3)$$

4) *Gradients:* The probability distribution $\mathbf{p}_k(t)$ can undergo drastic changes upon continuation of motion along control dimension k . The spatial gradient of $\mathbf{p}_k(t)$ encodes this propensity for change and is approximated by

$$\frac{\partial \mathbf{p}_k(t)}{\partial x_k} = \mathbf{p}_k(t_c) - \mathbf{p}_k(t_b)$$

where x_k is the component of robot’s displacement along control dimension k . The greater the difference between individual spatial gradients, the greater will the probabilities deviate from each other, thereby helping in disambiguation. In order to quantify the “spread” of gradients we define a quantity Υ_k

$$\Upsilon_k = \sum_{i=1}^{n_g} \sum_{j=i}^{n_g} \left| \frac{\partial p_k^i(t)}{\partial x_k} - \frac{\partial p_k^j(t)}{\partial x_k} \right| \quad (4)$$

where $|\cdot|$ denotes the absolute value.

Putting it all together: Γ_k , Ω_k , Λ_k and Υ_k are then combined to compute D_k as

$$D_k = \underbrace{w \cdot (\Gamma_k \cdot \Omega_k \cdot \Lambda_k)}_{\text{short-term}} + \underbrace{(1 - w) \cdot \Upsilon_k}_{\text{long-term}} \quad (5)$$

where w is a task-specific weight that balances the contributions of the short-term and long-term components. (In our implementation, $w = 0.5$.) Equation 5 actually is computed twice, once in each of the positive (\mathbf{e}^k) and negative directions ($-\mathbf{e}^k$) along k , and the results (D_k^+ and D_k^-) are then summed. The computation of D_k is performed for each control dimension $k \in \mathcal{K}$.

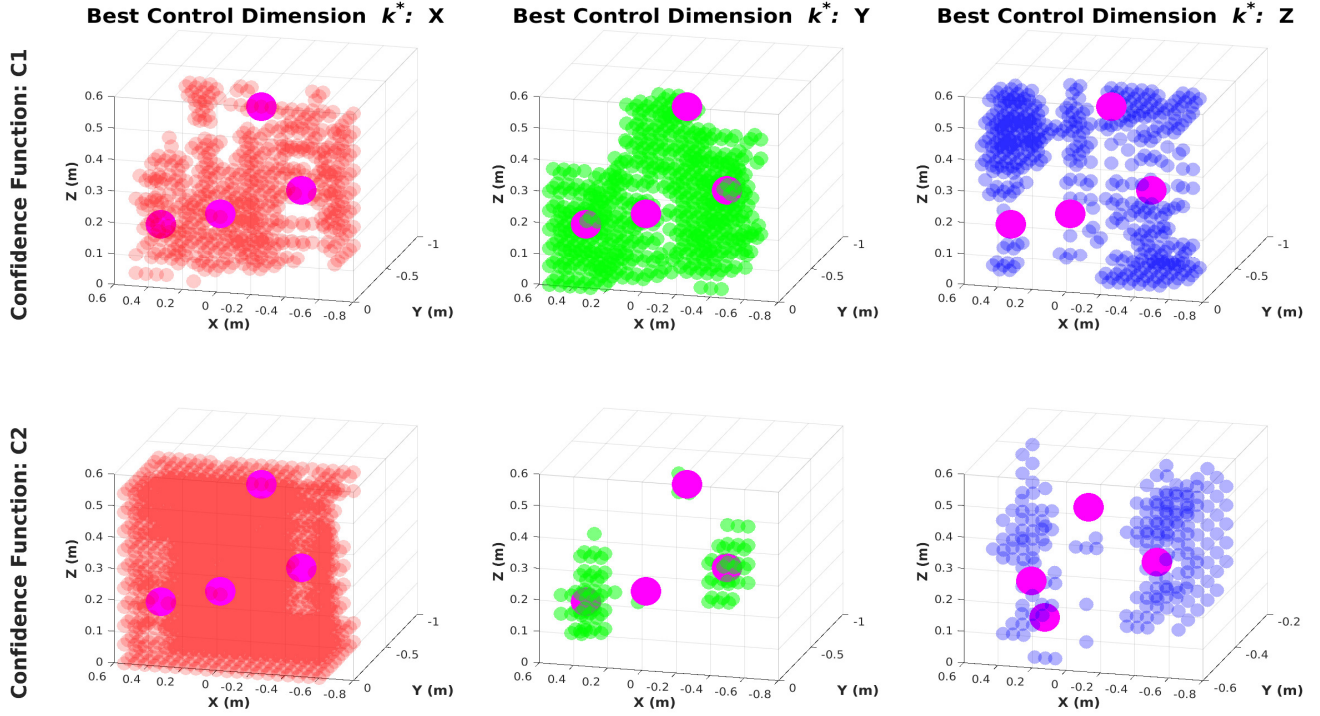


Fig. 4 Control dimensions best able to disambiguate intent. Left column: k^* is X. Middle Column: k^* is Y. Right Column: k^* is Z. Magenta spheres indicate the goal locations (intent). In this example, the goals are spread maximally along the x and z dimensions, and so inference happens more quickly if the human control commands are along x or z . We see that x and z are chosen more often as the most disambiguating dimensions when using intent inference function C2 (bottom row). Function C2 considers the instantaneous directedness of the human’s control command towards that goal, while inference function C1 (top row) encodes only proximity to a given goal. Function C2 is considered to encode more information about the human’s intent than C1, with the result of stronger inference power—which is inherently linked to the disambiguation power of our algorithm. Further details in (Gopinath and Argall 2017).

The disambiguation metric D_m for control mode m then is calculated as

$$D_m = \sum_k D_k$$

where $k \in m$ iterates through the set of control dimensions on which m is able to operate. Lastly, the control mode with highest disambiguation capability m^* is given by

$$m^* = \operatorname{argmax}_m D_m$$

while $k^* = \operatorname{argmax}_k D_k$ gives the control dimension with highest disambiguation capability k^* . Disambiguation mode m^* is the mode that the algorithm chooses for the human to better estimate their intent. Any control command issued by the user in m^* is likely to be more useful for the robot in determining which is the human’s intended goal, because of the maximal confidence disambiguation.

3.3 Intent Inference

This section describes the intent inference scheme used in this paper. Our preliminary work (Gopinath and Argall 2017) revealed that the power of our disambiguation algorithm proposed in Section 3.2 is intimately linked with the inference power of different choices of intent inference mechanisms. More importantly, the pilot study associated with this preliminary work suggested that incorporating a history of past states and actions would improve performance. We therefore propose an extended disambiguation formulation which furthermore incorporates history.

In this work, we propose a novel intent inference scheme inspired by *dynamic field theory* in which the time evolution of the probability distribution $\mathbf{p}(t)$ is specified as a dynamical system with constraints. An alternate approach is to perform intent inference using Bayesian techniques, which in theory can take into account the influence of past states and actions. In practice, however, low-order Markov assumptions are usually

made to make the inference tractable computationally, and with such assumptions history is lost.

Section 3.3.1 provides a primer on the basic principles and features of *dynamic field theory* and its application in the fields of neuroscience and cognitive robotics. Section 3.3.2 describes our novel formulation that makes use of dynamic field theory for the purposes of intent inference.

3.3.1 Dynamic Field Theory

In Dynamic Field Theory (DFT) (Schöner and Spencer 2015), variables of interest are treated as dynamical state variables. To represent the information about these variables requires two dimensions: one which specifies the value the variables can attain (the domain) and the other which encodes the *activation level* or the amount of information about that a particular value. These *activation fields* are analogous to probability distributions defined over a random variable.

Following Amari’s formulation (Amari 1977) dynamics of an activation field $\phi(x, t)$ are given by

$$\tau \dot{\phi}(x, t) = -\phi(x, t) + h + S(x, t) + \int dx' b(x - x') \sigma(\phi(x', t))$$

where x denotes the variable of interest, t is time, τ is the time-scale parameter, h is the constant resting level, and $S(x, t)$ is the external input, $b(x - x')$ is the interaction kernel and $\sigma(\phi)$ is a sigmoidal nonlinear threshold function. The interaction kernel mediates how activations at all other field sites x' drive the activation level at x . Two types of interactions are possible: excitatory (when interaction is positive) which drives up the activation, and inhibitory (when the interaction is negative) which drives the activation down. Historically, dynamic neural fields originally were conceived to explain cortical population neuronal dynamics, based on the hypothesis that the excitatory and inhibitory neural interactions between local neuronal pools form the basis of cortical information processing (Wilson and Cowan 1973).

Dynamic neural fields possess some unique characteristics that make them ideal candidates for modeling higher-level cognition. First, a peak in the activation field can be *sustained* even in the absence of external input due to the recurrent interaction terms. Second, information from the past can be *preserved* over much larger time scales quite easily by tuning the time-scale parameter thereby endowing the fields with memory. Third, the activation fields are *robust* to disturbance and noise in the external output (Schöner 2008). As a result, DFT principles have found widespread application

in the area of cognitive robotics (Erlhagen and Bicho 2006), specifically in the contexts of efficient human-robot interaction (Erlhagen and Bicho 2014), robotic scene representation (Zibner et al 2011), obstacle avoidance and target reaching behaviors in both humans and robots (Schöner et al 1995), and for object learning and recognition (Faubel and Schöner 2008).

3.3.2 Dynamic Neural Fields for Intent Inference

Recurrent interaction between the state variables, robustness to noise and inherent memory make dynamic neural fields an ideal candidate for an intent inference engine. Our insight is to use the framework of dynamic neural fields to specify the time evolution of the probability distribution $\mathbf{p}(t)$, in which we treat the individual goal probabilities $p^i(t)$ as constrained dynamical state variables such that $p^i(t) \in [0, 1]$ and $\sum_1^{n_g} p^i(t) = 1$. The dynamical system can be generically written as

$$\dot{\mathbf{p}}(t) = F(\mathbf{p}(t), \mathbf{u}_h; \Theta)$$

where F represents the nonlinear vector field, \mathbf{u}_h is the human control input and Θ represents all other task-relevant features and parameters that affect the time-evolution of the probability distribution. The full specification of the neural field is given by

$$\frac{\partial \mathbf{p}(t)}{\partial t} = \frac{1}{\tau} \left[-\mathbb{I}_{n_g \times n_g} \cdot \mathbf{p}(t) + \underbrace{\frac{1}{n_g} \cdot \mathbb{1}_{n_g}}_{\text{rest state}} + \underbrace{\boldsymbol{\lambda}_{n_g \times n_g} \cdot \sigma(\boldsymbol{\xi}(\mathbf{u}_h; \Theta))}_{\text{excitatory} + \text{inhibitory}} \right] \quad (6)$$

where time-scale parameter τ determines the memory capacity of the system, $\mathbb{I}_{n_g \times n_g}$ is the identity matrix, $\mathbb{1}_{n_g}$ is a vector containing all ones of dimension n_g , $\boldsymbol{\lambda}$ is the control matrix that controls the excitatory and inhibitory aspects, $\boldsymbol{\xi}$ is a function that encodes the non-linearity through which human control commands and task features affect the time evolution, and σ is a bi-ased sigmoidal nonlinearity given by $\sigma(\boldsymbol{\xi}) = \frac{1}{1+e^{-\boldsymbol{\xi}}} - 0.5$. The off-diagonal elements of $\boldsymbol{\lambda}$ mediate the interaction between all of the probabilities. In the absence of any information or cues, the probability distribution settles to a resting state which is a uniform distribution, that is whenever $\mathbf{u}_h = 0$, $\boldsymbol{\xi} = \mathbf{0}$. Given the initial probability distribution at time t_a Equation 6 can be solved numerically from $t \in [t_a, t_b]$ using a simple Euler algorithm with a fixed time-step Δt .

The design of $\boldsymbol{\xi}$ is informed by what features of the human control input and environment capture the human’s underlying intent most effectively. We rely on the *directedness* of the human control commands towards

a goal, the *proximity* to a goal and the *agreement* between the human commands and robot autonomy. With $\Theta = \{\mathbf{x}_r, \mathbf{x}_{g^i}, \mathbf{u}_{r,g^i}\}$, one dimension i of ξ is defined as

$$\xi^i(\mathbf{u}_h; \mathbf{x}_r, \mathbf{x}_{g^i}, \mathbf{u}_{r,g^i}) = \underbrace{\frac{1+\eta}{2}}_{\text{directedness}} + \underbrace{\mathbf{u}_h^{\text{rot}} \cdot \mathbf{u}_{r,g^i}^{\text{rot}}}_{\text{agreement}} + \underbrace{\max\left(0, 1 - \frac{\|\mathbf{x}_{g^i} - \mathbf{x}_r\|}{R}\right)}_{\text{proximity}}$$

where $\eta = \frac{\mathbf{u}_h^{\text{trans}} \cdot (\mathbf{x}_{g^i} - \mathbf{x}_r)^{\text{trans}}}{\|\mathbf{u}_h^{\text{trans}}\| \|(\mathbf{x}_{g^i} - \mathbf{x}_r)^{\text{trans}}\|}$, \mathbf{u}_{r,g^i} is the robot autonomy command for reaching goal g^i , *trans* and *rot* refer to the translational and rotational components of a command \mathbf{u} or position \mathbf{x} , R is the radius of the sphere beyond which the proximity component is always zero, and $\|\cdot\|$ is the Euclidean norm. That is, in the absence of any human control command, the probability distribution decays to the resting state which is a uniform distribution. The most confident goal g^* then is computed as

$$g^* = \underset{i}{\operatorname{argmax}} p^i(t) \quad (7)$$

At every time step the constraints on $p^i(t)$ are enforced thereby ensuring that $\mathbf{p}(t)$ is a valid probability distribution at all times.

4 Shared Control

The shared control paradigm implemented on our robot is a blending-based approach in which the final control command issued to the robot is a linear composition of the human control command and an autonomous robot policy. The autonomous control policy generates control command $\mathbf{u}_r \leftarrow f_r(\mathbf{x})$ where $f_r(\cdot) \in \mathcal{F}_r$, and \mathcal{F}_r is the set of all control behaviors corresponding to different tasks. This set could be derived using a variety of techniques such as *Learning from Demonstrations* (Argall et al 2009; Schaal 1997), motion planners (Hsu et al 2002; Ratliff et al 2009) or navigation functions (Rimon and Koditschek 1992; Tanner et al 2003). Specifically, let $\mathbf{u}_{r,g}$ be the autonomy command associated with goal g . The final control command \mathbf{u} issued to the robot then is given by

$$\mathbf{u} = \alpha \cdot \mathbf{u}_{r,g^*} + (1 - \alpha) \cdot \mathbf{u}_h$$

where g^* is the most confident goal. The blending factor α is a piecewise linear function of the probability $p(g^*)$ associated with g^* and is given by

$$\alpha = \begin{cases} 0 & p(g^*) \leq \rho_1 \\ \frac{\rho_3}{\rho_2 - \rho_1} \cdot p(g^*) & \text{if } \rho_1 < p(g^*) \leq \rho_2 \\ \rho_3 & p(g^*) > \rho_2 \end{cases}$$

with $\rho_i \in [0, 1] \forall i \in [1, 2, 3]$ and $\rho_2 > \rho_1$. In our implementation, we empirically set $\rho_1 = \frac{1.2}{n_g}$, $\rho_2 = \frac{1.4}{n_g}$ and $\rho_3 = 0.7$. Each location $\mathbf{x} \in \mathbb{R}^3 \times \mathbb{S}^3$ consists of a position component (3 dimensions) and orientation component (represented as a quaternion in 4 dimensions).⁴ Each control command $\mathbf{u} \in \mathbb{R}^6$ consists of a translational velocity component (3 dimensions) and rotational velocity component expressed as Euler rates (3 dimensions).

The robot control command $\mathbf{u}_{r,g}$ is generated using a simple potential field which is defined in all parts of the state space (Khatib 1986). Every goal g is associated with a potential field γ_g which treats g as an attractor and all the other goals in the scene as repellers. For potential field γ_g , the attractor velocity is given by

$$\dot{\mathbf{x}}_r^{\text{attract}} = \mathbf{x}_g - \mathbf{x}_r$$


where \mathbf{x}_g is the location of goal g .⁵ The repeller velocity is given by

$$\dot{\mathbf{x}}_r^{\text{repel}} = \sum_{i \in \mathcal{G} \setminus g} \frac{\mathbf{x}_r - \mathbf{x}_{g^i}}{\mu(\|\mathbf{x}_r - \mathbf{x}_{g^i}\|^2)}$$

where $\dot{\mathbf{x}}_r$ indicates the velocity of the robot in the world frame, μ controls the magnitude of the repeller velocity and $\|\cdot\|$ is the Euclidean norm. The autonomy command is computed as a summation of these attractor and repeller velocities.

$$\mathbf{u}_{r,g} = \dot{\mathbf{x}}_r^{\text{attract}} + \dot{\mathbf{x}}_r^{\text{repel}}$$

γ_g operates in the full six dimensional Cartesian space, and treats position and orientation as independent potential fields.



Control Mappings		
Mode	Head Array	Joystick
1	v_x	v_x, v_y
2	v_y	v_x, v_z
3	v_z	ω_z, ω_y
4	ω_z	ω_x
5	ω_y	—
6	ω_x	—

Fig. 5 A 2-axis joystick (left) and switch-based head array (center) and their operational paradigms (right). v and ω indicate the translational and rotational velocities of the end-effector, respectively.

⁴ \mathbb{S}^3 is the space of all unit quaternions.

⁵In position space, the ‘ $-$ ’ operator computes the difference between the goal position and current robot position in \mathbb{R}^3 . In orientation space, the ‘ $-$ ’ operator computes the *quaternion difference* between the goal orientation and the current robot orientation.

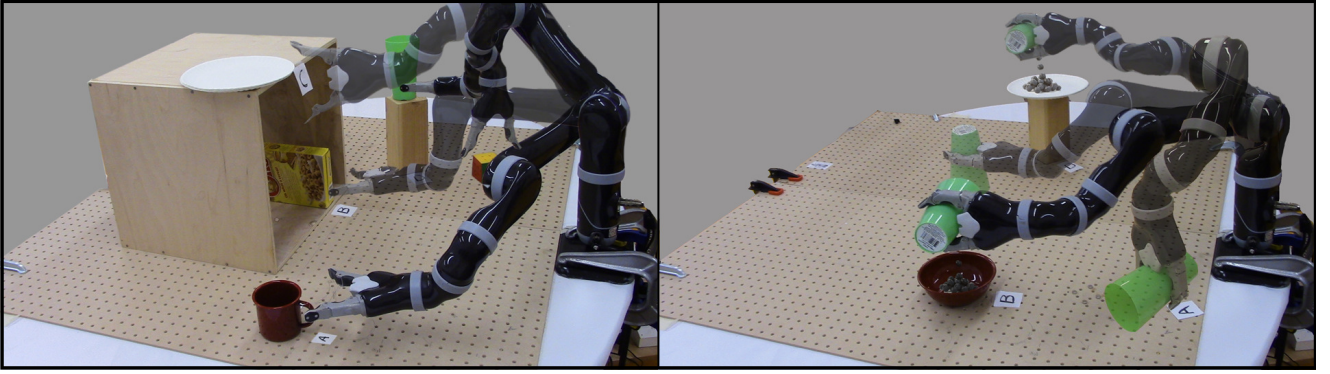


Fig. 6 Study tasks performed by subjects. *Left:* Single-step reaching task. *Right:* Multi-step Pouring task.

5 Study Methods

In this section, we describe the study methods used to evaluate the efficacy of the disambiguation system.

5.1 Participants

For this study eight subjects were recruited (mean age: 31 ± 11 , 3 males and 5 females). All participants gave their informed, signed consent to participate in the experiment, which was approved by Northwestern University’s Institutional Review Board.

5.2 Hardware

The experiments were performed using the MICO 6-DoF robotic arm (Kinova Robotics, Canada), specifically designed for assistive purposes. The software system was implemented using the Robot Operating System (ROS) and data analysis was performed in MATLAB.

The subjects teleoperated the robot using two different control interfaces: a 2-axis joystick and a switch-based head array. The control signals captured from the interfaces were mapped to the Cartesian velocities of the end-effector (Figure 5).

The joystick generated continuous control signals and allowed for control of a maximum of two dimensions at a time. The 6-D control space was partitioned into four control modes that could be accessed using the buttons on the joystick interface. The switch-based head array consisted of three switches embedded in the headrest and generated 1-D discrete signals. The switch at the back of the headrest was used to cycle between the different control modes, and the switches to the left and right controlled the motion of the robot’s end effector in the positive and negative directions along the dimension corresponding to the selected control mode. All switches were operated via head movements. An external button

was provided to request the mode switch assistance. For both control interfaces the gripper had a dedicated control mode.

5.2.1 Switching Paradigms

Two kinds of mode switching paradigms were evaluated in the study. Note that the blending assistance was always active for both paradigms. Under the blending paradigm, the amount of assistance was directly proportional to the probability of the most confident goal g^* , and thus to the strength of the intent inference. Therefore, if intent inference improved as a result of goal disambiguation, more assistance would be provided by the robot. All trials started in a randomized initial control mode and robot position.

Manual: During task execution the user performed all mode switches.

Disambiguation: The user additionally could request a disambiguation mode switch at any time during task execution. Upon disambiguation request, the algorithm identified and switched the current control mode to the best disambiguating mode m^* . The user was required to request disambiguation at least once during the task execution.

5.3 Study Protocol

A within-subjects study was conducted using a fractional factorial design in which the manipulated variables were the tasks, control interfaces and the switching paradigm conditions. Each subject underwent an initial training period that lasted approximately thirty minutes after which the subject performed both tasks using both interfaces under the *Manual* and *Disambiguation* paradigms. The trials were balanced and the control interfaces and the paradigms were randomized and counterbalanced across all subjects to avoid ordering effects. Three trials

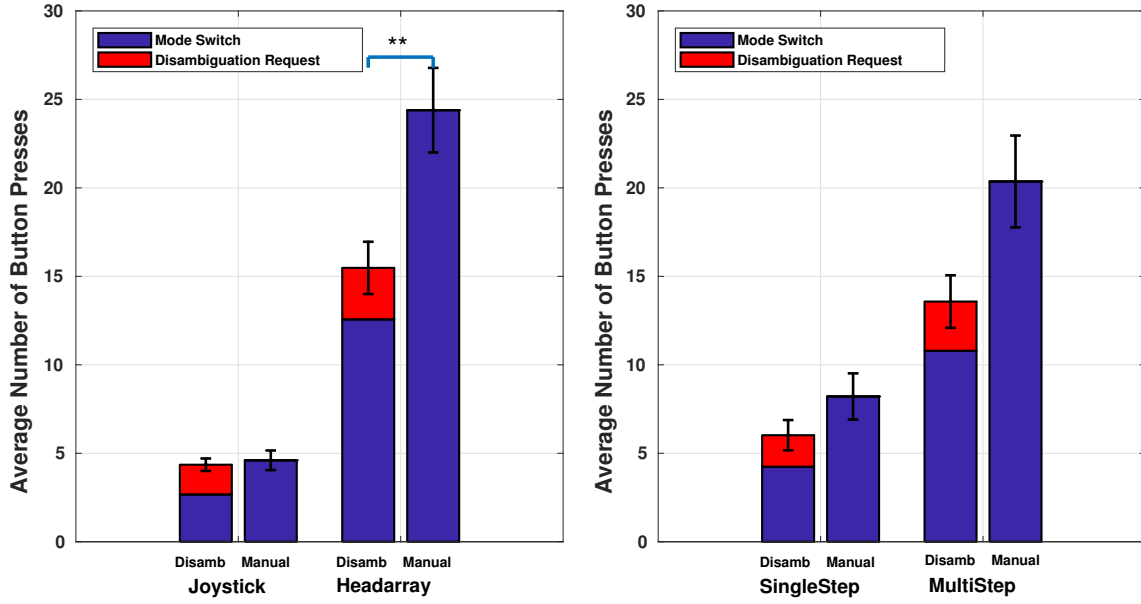


Fig. 7 Comparison of average number of button presses between *Disambiguation* and *Manual* Paradigms. *Left*: Grouped by control interfaces. *Right*: Grouped by tasks.

were collected for the *Manual* paradigm and five trials for the *Disambiguation* paradigm.

Training: The training period consisted of three phases and two different task configurations. The subjects used both interfaces to perform the training tasks.

Phase One: The subjects were asked to perform a simple reaching motion towards a single goal in the scene. This phase was intended for the subjects to get familiarized with the control interface mappings and teleoperation of the robotic arm.

Phase Two: In the second phase of training, the blending-based shared autonomy was introduced. The subjects experienced how the autonomy could provide assistance during the task execution. The subjects were informed that the robot autonomy would be present for all trials of the experiment.

Phase Three: For the third phase of the training, multiple objects were introduced in the scene. Subjects were informed that the robot had the capability to pick a control mode that would help it figure out which goal they were going for, and that the subject had the option to request the robot to pick that control mode. Subjects were able to explore this request feature during a reaching task, and were instructed to move as much as s/he can in the control mode chosen by the robot and observe the effects of the mode switch request.

Testing: Two different task types were evaluated during testing. Both control interfaces were employed, for all tasks.

Single-step: The task is to reach one of five objects on the table, each with a target orientation (Figure 6, Left).

Multi-step: Each trial began with a full cup held by the robot gripper. The task required first that the contents of the cup be poured into one of two containers and then that the cup be placed at one of the two specified locations and with a specific orientation (Figure 6, Right).

Metrics: The objective metrics used for evaluation include the following. *Number of mode switches* refers to the number of times a user switched between various control modes during task execution. *Number of disambiguation requests* refers to the number of times user pressed the button requesting disambiguating assistance. *Number of button presses* is the sum of *Number of mode switches* and *Number of disambiguation requests*, and is also an indirect measure of user effort. *Onset of robot assistance* refers to the earliest time at which blending assistance to became active. We also characterize the temporal distribution of disambiguation requests using a skewness measure.

6 Results

Here we report the results of our subject study. Statistical significance was determined by the Wilcoxon Rank-Sum test in where (***) indicates $p < 0.001$, (**) $p < 0.01$ and (*) $p < 0.05$.

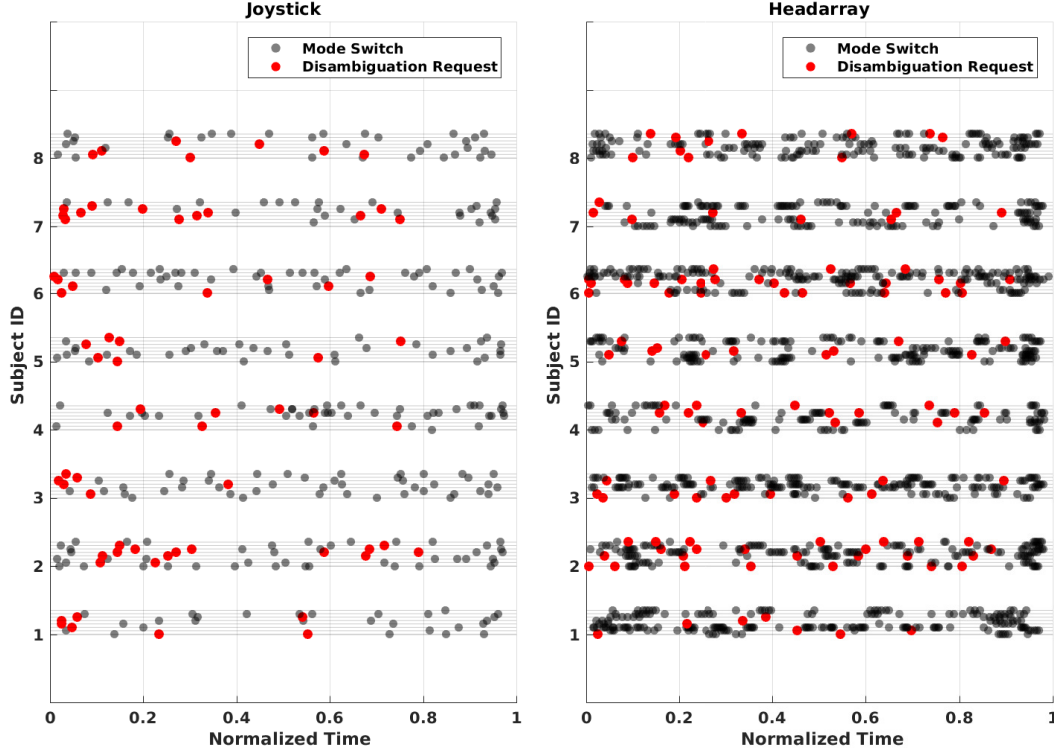


Fig. 8 Temporal pattern of button presses for each interface and the multi-step task on a trial-by-trial basis for all subjects. Eight trials per subject per interface/task combination.

6.1 Impact of Disambiguation on Task Performance

Figure 7 presents the number of button presses under each mode switching paradigm, for both interfaces and tasks.

A statistically significant decrease in the number of button presses was observed between the *Manual* and *Disambiguation* paradigms when using the headarray (Figure 7, Left). Due to the low-dimensionality of headarray and cyclical nature of mode switching, the number of button presses required for task completion is inherently high. That the disambiguation paradigm was helpful in reducing the number of button presses likely is due to the fact that robot assistance was more effective in the disambiguating control mode and therefore reduced the need for subsequent user-initiated mode switches.

For joystick, statistically significant differences were observed for the number of mode switches between the two paradigms ($p < 0.05$, not pictured in Figure 7). However, the gain due to the reduction of user-initiated mode switches was offset by the button presses that were required for disambiguation requests.

A general trend (although not statistically significant) of a decrease in the number of button presses

Table 1 Characterization of the temporal distribution of disambiguation requests. The values in the table denote the deviation of the temporal distribution from a uniform distribution. Smaller values mean more concentrated and earlier disambiguation requests.

	Single Step	Multi Step
Joystick	0.63	0.57
Headarray	0.35	0.22

was also observed for the more complex multi-step task (Figure 7, Right).

These results suggest that disambiguation has a greater effect as the control interface becomes more limited and the task becomes more complex.

6.2 Temporal Distribution of Disambiguation Requests

We also observed similar trends in the *temporal distribution* of disambiguation requests, where a higher number of disambiguation requests correlates with the more limited interface and complex task. The temporal distribution of disambiguation requests refers to *when* the subject requested assistance during the course of a trial. We use a measure of *skewness* to characterize how

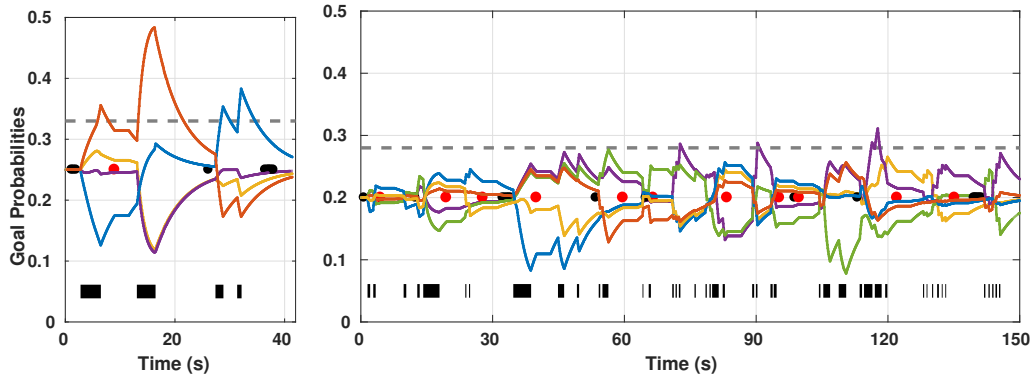


Fig. 9 Time evolution of goal probabilities. *Top*: Multi-step task. *Bottom*: Single-step task. The gray horizontal line above denotes the minimum threshold for robot assistance. The black bars at the bottom denote non-zero human control commands. The red and black dots indicate button presses that are disambiguation requests and mode switches respectively.

much the temporal distribution deviates from a uniform distribution.⁶ Larger positive values of skewness correlate with more concentrated and earlier disambiguation requests. Table 1 reports the skewness of the temporal distribution of disambiguation requests for different interface-task combinations.

Figure 8 shows the temporal pattern of disambiguation requests and mode switches for the multi-step task on a trial-by-trial basis for all subjects. From the figure it is clear that the frequency and density of button presses (disambiguation requests plus mode switches) are much higher for the more limited control interface. The subjects also demonstrated a diverse range of disambiguation request behavior, for example in regards to both when during the execution requests were made and with what frequency (e.g. Subject 8 versus Subject 2, Joystick). The variation between subjects is likely due to different factors such as the user’s comfort in operating the robot and understanding the ability of the disambiguating mode to recruit more assistance from the autonomy.

6.3 Onset of Robot Assistance

Our motivating intuition for developing the disambiguation system was that disambiguation should allow the autonomy to step in earlier during the course of task execution. However, our results did not reveal any differences between the two switching paradigms across tasks or across interfaces (Figure 10).

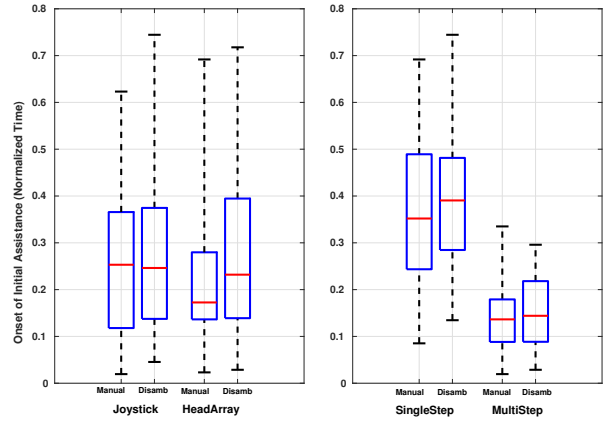


Fig. 10 Onset of robot assistance normalized with respect to task completion time. *Left*: Across interfaces. *Right*: Across tasks.

One likely contributing factor is that disambiguation frequently was impaired by subjects surprisingly choosing not to operate in the disambiguation mode after making a disambiguation request. The disambiguation power of a control mode depends entirely on the observation of motion within that mode, and so in such scenarios disambiguation is effectively rendered inert.

This phenomenon is illustrated in Figure 9. When control commands are issued, they are indicated by the black bars on the bottom of the plots. Disambiguation requests are shown as red dots, and mode switches as black dots. In the right plot, we see multiple instances of disambiguation requests being followed by no control commands or only very brief control commands. Another interesting behavior is shown in the left plot, where operation in the disambiguating mode very quickly elevates one goal probability above the threshold for providing

⁶A uniform temporal distribution corresponds to a trial in which the disambiguation requests are uniformly spread out during the course of task execution. The skewness of a uniform distribution is 0.

autonomy assistance, and after the assistance kicks in the subject elects to stop issuing control commands.

7 Discussion

In a *help me, help you* type of human robot system, task execution becomes seamless and more efficient when there is a sound mutual understanding of how the other party operates. One surprising observation from our subject study was how often participants submitted a disambiguation request, and then chose not to operate in the selected mode—effectively not helping the robot help them. Of course one possible explanation is that subjects found the disambiguation mode to be in conflict with how they wanted to operate the robot. However another plausible explanation is simply a lack of understanding of how they might help the robot help them. In order to provide *intent-expressive* control commands to the robot, very likely knowledge of the assistance mechanism is critical.

Therefore, the need for extensive and thorough training becomes apparent. The training can be made more effective in a few different ways. First, online feedback of the robot’s intent prediction at all times during training can likely help the subject gain a better understanding of the relationship between the characteristics of their control actions (sparsity, aggressiveness, persistence) and the robot’s assistive behavior. Second, the subjects could be explicitly informed of the task relevant features (directedness, proximity *et cetera*) that the robot relies on for determining the amount of assistance. Knowledge of these features might motivate the users to leverage the disambiguating mode.

The inherent time delays associated with the computation of the disambiguating mode (approximately 2-2.5s) might have been a discouraging factor and a cause for user frustration. The algorithm could be used to pre-compute a large set of most informative modes for different parts of the workspace, for different goal configurations and for different priors ahead of time, which then might be used a lookup table during task execution. Furthermore, metamodeling techniques and machine learning tools can be used to learn generalizable models that will be effective in previously unseen goal configurations.

In the present system, there is task effort associated with requesting disambiguation assistance which can discourage the users from utilizing the paradigm. Automated mode switching schemes can possibly eliminate the need for button presses for disambiguation requests. We also identify an opportunity to have adaptive assistance paradigms that explicitly take into account the characteristics of the user’s control behavior. Some users

are timid in their operation of the robot whereas some others are more aggressive and confident. Some are more comfortable operating the robot manually and do not seek assistance, whereas some others rely on assistance more frequently. Individual user characteristics could be extracted from training and be used for tuning the parameters of the intent inference engine and the shared control system to maximize robustness and efficacy of the assistive system. This would also likely improve user satisfaction and result in higher user acceptance.

8 Conclusion

In this paper, we have presented an algorithm for *intent disambiguation assistance* with a shared-control robotic arm using the notion of *inverse legibility*. The goal of our algorithm is to elicit more *intent-expressive* control commands from the user by placing control in those control modes that *maximally disambiguate* between the various goals in the scene. As a secondary contribution, we also present a novel intent inference mechanism inspired by *dynamic field theory* that works in conjunction with the disambiguation system. Pilot user study was conducted with eight subjects to evaluate the efficacy of the disambiguation system. Our results indicate a decrease in task effort in terms of the number of button presses when disambiguation system employed. In our future work, as informed by our pilot study, we plan to extend the framework into an automated mode switch assistance system. A more extensive user study with motor-impaired subjects will also be conducted in the future to further evaluate the utility of the disambiguation system and explore the disambiguation request patterns of users.

References

- Amari Si (1977) Dynamics of pattern formation in lateral-inhibition type neural fields. *Biological Cybernetics* 27(2):77–87
- Argall BD, Chernova S, Veloso M, Browning B (2009) A survey of robot learning from demonstration. *Robotics and Autonomous Systems* 57(5):469–483
- Atanasov N, Le Ny J, Daniilidis K, Pappas GJ (2014) Information acquisition with sensing robots: Algorithms and error bounds. In: *Proceedings of the IEEE International Conference on Robotics and Automation (ICRA)*
- Baker CL, Tenenbaum JB, Saxe RR (2007) Goal inference as inverse planning. In: *Proceedings of the Cognitive Science Society*
- Baker CL, Saxe RR, Tenenbaum JB (2009) Action understanding as inverse planning. *Cognition* 113(3):329–349
- Choi YS, Anderson CD, Glass JD, Kemp CC (2008) Laser pointers and a touch screen: intuitive interfaces for autonomous mobile manipulation for the motor impaired. In:

- Proceedings of the International SIGACCESS Conference on Computers and Accessibility*
- Demeester E, Hüntemann A, Vanhooydonck D, Vanacker G, Van Brussel H, Nuttin M (2008) User-adapted plan recognition and user-adapted shared control: A bayesian approach to semi-autonomous wheelchair driving. *Autonomous Robots* 24(2):193–211
- Downey JE, Weiss JM, Muelling K, Venkatraman A, Valois JS, Hebert M, Bagnell JA, Schwartz AB, Collinger JL (2016) Blending of brain-machine interface and vision-guided autonomous robotics improves neuroprosthetic arm performance during grasping. *Journal of Neuroengineering and Rehabilitation* 13(1):28
- Dragan AD, Srinivasa SS (2012) Assistive teleoperation for manipulation tasks. In: *Proceedings of ACM/IEEE International Conference on Human-Robot Interaction (HRI)*
- Dragan AD, Lee KC, Srinivasa SS (2013) Legibility and predictability of robot motion. In: *Proceedings of the ACM/IEEE International Conference on Human-Robot Interaction (HRI)*
- Driessen B, Kate TT, Liefhebber F, Versluis A, Van Woerden J (2005) Collaborative control of the manus manipulator. *Universal Access in the Information Society* 4(2):165–173
- Eftiring H, Boschian K (1999) Technical results from manus user trials. In: *IEEE 2nd International Conference on Rehabilitation Robotics (ICORR)*
- Erlhagen W, Bicho E (2006) The dynamic neural field approach to cognitive robotics. *Journal of Neural Engineering* 3(3):R36
- Erlhagen W, Bicho E (2014) A dynamic neural field approach to natural and efficient human-robot collaboration. In: *Neural Fields*, Springer, pp 341–365
- Faubel C, Schöner G (2008) Learning to recognize objects on the fly: a neurally based dynamic field approach. *Neural Networks* 21(4):562–576
- Goodfellow IJ, Koenig N, Muja M, Pantofaru C, Sorokin A, Takayama L (2010) Help me help you: Interfaces for personal robots. In: *Proceedings of ACM/IEEE International Conference on Human-Robot Interaction (HRI)*
- Gopinath D, Argall B (2017) Mode switch assistance to maximize human intent disambiguation. In: *Robotics: Science and Systems*
- Gopinath D, Jain S, Argall BD (2017) Human-in-the-loop optimization of shared autonomy in assistive robotics. *IEEE Robotics and Automation Letters* 2(1):247–254
- Herlant LV, Holladay RM, Srinivasa SS (2016) Assistive teleoperation of robot arms via automatic time-optimal mode switching. In: *Proceedings of the ACM/IEEE International Conference on Human-Robot Interaction (HRI)*
- Holladay RM, Dragan AD, Srinivasa SS (2014) Legible robot pointing. In: *The IEEE International Symposium on Robot and Human Interactive Communication (RO-MAN)*
- Hsu D, Kindel R, Latombe JC, Rock S (2002) Randomized kinodynamic motion planning with moving obstacles. *The International Journal of Robotics Research* 21(3):233–255
- Huete AJ, Victores JG, Martinez S, Giménez A, Balaguer C (2012) Personal autonomy rehabilitation in home environments by a portable assistive robot. *IEEE Transactions on Systems, Man, and Cybernetics, Part C (Applications and Reviews)* 42(4):561–570
- Kelley R, Tavakkoli A, King C, Nicolescu M, Nicolescu M, Bebis G (2008) Understanding human intentions via hidden markov models in autonomous mobile robots. In: *Proceedings of the 3rd ACM/IEEE International Conference on Human Robot Interaction*, ACM, pp 367–374
- Khatib O (1986) Real-time obstacle avoidance for manipulators and mobile robots. *The International Journal of Robotics Research* 5(1):90–98
- Kim DJ, Hazlett R, Godfrey H, Rucks G, Portee D, Bricout J, Cunningham T, Behal A (2010) On the relationship between autonomy, performance, and satisfaction: Lessons from a three-week user study with post-sci patients using a smart 6dof assistive robotic manipulator. In: *Proceedings of the IEEE International Conference on Robotics and Automation (ICRA)*, IEEE, pp 217–222
- Kim DJ, Hazlett-Knudsen R, Culver-Godfrey H, Rucks G, Cunningham T, Portee D, Bricout J, Wang Z, Behal A (2012) How autonomy impacts performance and satisfaction: Results from a study with spinal cord injured subjects using an assistive robot. *IEEE Transactions on Systems, Man, and Cybernetics-Part A: Systems and Humans* 42(1):2–14
- LaPlante MP, et al (1992) Assistive technology devices and home accessibility features: prevalence, payment, need, and trends. *Advance Data from Vital and Health Statistics*
- Liu C, Hamrick JB, Fisac JF, Dragan AD, Hedrick JK, Sastry SS, Griffiths TL (2016) Goal inference improves objective and perceived performance in human-robot collaboration. In: *Proceedings of the 2016 International Conference on Autonomous Agents & Multiagent Systems*, International Foundation for Autonomous Agents and Multiagent Systems, pp 940–948
- Miller LM, Murphey TD (2013) Trajectory optimization for continuous ergodic exploration. In: *American Control Conference (ACC)*
- Miller LM, Silverman Y, MacIver MA, Murphey TD (2016) Ergodic exploration of distributed information. *IEEE Transactions on Robotics* 32(1):36–52
- Muelling K, Venkatraman A, Valois JS, Downey JE, Weiss J, Javdani S, Hebert M, Schwartz AB, Collinger JL, Bagnell JA (2017) Autonomy infused teleoperation with application to brain computer interface controlled manipulation. *Autonomous Robots* pp 1–22
- Nuttin M, Vanhooydonck D, Demeester E, Van Brussel H (2002) Selection of suitable human-robot interaction techniques for intelligent wheelchairs. In: *Proceedings of 11th IEEE International Workshop on Robot and Human Interactive Communication*, IEEE, pp 146–151
- Philips J, Millán JdR, Vanacker G, Lew E, Galán F, Ferrez PW, Van Brussel H, Nuttin M (2007) Adaptive shared control of a brain-actuated simulated wheelchair. In: *Proceedings of the IEEE International Conference on Rehabilitation Robotics (ICORR)*, IEEE, pp 408–414
- Pilarski PM, Dawson MR, Degris T, Carey JP, Sutton RS (2012) Dynamic switching and real-time machine learning for improved human control of assistive biomedical robots. In: *Proceedings of the IEEE RAS & EMBS International Conference on Biomedical Robotics and Biomechanics (BioRob)*, IEEE, pp 296–302
- Ratliff N, Zucker M, Bagnell JA, Srinivasa S (2009) Chomp: Gradient optimization techniques for efficient motion planning. In: *Proceedings of the IEEE International Conference on Robotics and Automation (ICRA)*, IEEE, pp 489–494
- Rimon E, Koditschek DE (1992) Exact robot navigation using artificial potential functions. *IEEE Transactions on Robotics and Automation* 8(5):501–518
- Sadigh D, Sastry S, Seshia SA, Dragan AD (2016a) Planning for autonomous cars that leverage effects on human actions. In: *Robotics: Science and Systems*
- Sadigh D, Sastry SS, Seshia SA, Dragan A (2016b) Information gathering actions over human internal state. In: *Proceedings of the IEEE/RSJ International Conference on*

- Intelligent Robots and Systems (IROS)*, IEEE, pp 66–73
- Schaal S (1997) Learning from demonstration. In: *Advances in Neural Information Processing Systems*, pp 1040–1046
- Scherer MJ (1996) Outcomes of assistive technology use on quality of life. *Disability and Rehabilitation* 18(9):439–448
- Schöner G (2008) Dynamical systems approaches to cognition. *Cambridge Handbook of Computational Cognitive Modeling* pp 101–126
- Schöner G, Spencer J (2015) *Dynamic thinking: A primer on dynamic field theory*. Oxford University Press
- Schöner G, Dose M, Engels C (1995) Dynamics of behavior: Theory and applications for autonomous robot architectures. *Robotics and Autonomous Systems* 16(2-4):213–245
- Simpson T, Broughton C, Gauthier MJ, Prochazka A (2008) Tooth-click control of a hands-free computer interface. *IEEE Transactions on Biomedical Engineering* 55(8):2050–2056
- Sorokin A, Berenson D, Srinivasa SS, Hebert M (2010) People helping robots helping people: Crowdsourcing for grasping novel objects. In: *Proceedings of the IEEE/RSJ International Conference on Intelligent Robots and Systems (IROS)*
- Storms JG, Tilbury DM (2014) Blending of human and obstacle avoidance control for a high speed mobile robot. In: *American Control Conference (ACC)*, IEEE, pp 3488–3493
- Taha T, Miró JV, Dissanayake G (2011) A pomdp framework for modelling human interaction with assistive robots. In: *Proceedings of the IEEE International Conference on Robotics and Automation (ICRA)*, IEEE, pp 544–549
- Tanner HG, Loizou SG, Kyriakopoulos KJ (2003) Nonholonomic navigation and control of cooperating mobile manipulators. *IEEE Transactions on Robotics and Automation* 19(1):53–64
- Tomasello M, Carpenter M (2007) Shared intentionality. *Developmental Science* 10(1):121–125
- Tomasello M, Moll H (2010) The gap is social: Human shared intentionality and culture. In: *Mind the Gap*, Springer, pp 331–349
- Tsui KM, Kim DJ, Behal A, Kontak D, Yanco HA (2011) I want that: Human-in-the-loop control of a wheelchair-mounted robotic arm. *Applied Bionics and Biomechanics* 8(1):127–147
- Wang Z, Mülling K, Deisenroth MP, Ben Amor H, Vogt D, Schölkopf B, Peters J (2013) Probabilistic movement modeling for intention inference in human–robot interaction. *The International Journal of Robotics Research* 32(7):841–858
- Wilson HR, Cowan JD (1973) A mathematical theory of the functional dynamics of cortical and thalamic nervous tissue. *Biological Cybernetics* 13(2):55–80
- Zibner SK, Faubel C, Iossifidis I, Schöner G (2011) Dynamic neural fields as building blocks of a cortex-inspired architecture for robotic scene representation. *IEEE Transactions on Autonomous Mental Development* 3(1):74–91